Atmospheric Science Letters

RMetS Royal Meteorological Society

RESEARCH ARTICLE OPEN ACCESS

Cold Pools Reduce the Impacts of Deforestation on Convection Initiation

Nicholas M. Falk | Gabrielle R. Leung | Leah D. Grant | Susan C. van den Heever

Department of Atmospheric Science, Colorado State University, Fort Collins, Colorado, USA

Correspondence: Nicholas M. Falk (nick.falk@colostate.edu)

Received: 3 June 2025 | **Revised:** 23 December 2025 | **Accepted:** 19 January 2026

ABSTRACT

The individual and synergistic impacts of cold pools and land surface heterogeneity on convection initiation are investigated. Idealized large eddy simulations of deep convection over the Amazon rainforest are conducted. Simulations test realistic and homogenized vegetation, along with realistic and suppressed low-level evaporation which eliminates cold pools. Updrafts are tracked to determine convection initiation locations. The aggregation of initiation locations is quantified with an organization index. Initiation locations are randomly distributed over homogeneous vegetation, with or without cold pools, demonstrating that cold pools have minimal impacts on initiation locations over homogeneous vegetation. With realistic vegetation, convection initiation is more frequent over forested than deforested areas due to favorable thermodynamics. Heterogeneous vegetation effectively aggregates initiation locations and precipitation compared to homogeneous vegetation, whereas cold pools disaggregate initiation locations and precipitation by propagating into deforested regions and initiating convection. Thus, cold pools partially counteract the effects of anthropogenically driven land surface heterogeneity.

1 | Introduction

Anthropogenic deforestation in rainforests such as the Amazon creates a heterogeneous land surface. Such heterogeneities can drive mesoscale circulations thereby impacting the distribution of convective clouds and rainfall (Chagnon et al. 2004; Durieux et al. 2003; Paccini and Schiro 2025; Souza et al. 2000; Wang et al. 2009). When land surfaces with different properties are adjacent on the mesoscale, studies have shown that moist convection is usually favored over warmer, drier surfaces compared to nearby cooler, moister surfaces (Chagnon et al. 2004; Mascart et al. 1991; Rabin et al. 1990; Taylor et al. 2012). Enhanced convective activity over warm, dry surfaces has been attributed to mesoscale solenoidal circulations driven by surface heterogeneity (hereafter simply solenoidal circulations). These circulations flow at low levels from cool, moist regions into warm, dry regions, ascend in warm, dry regions, and then return toward cool, moist regions at higher levels. Ascent from solenoidal circulations can initiate convection in warm, dry regions (Branch and Wulfmeyer 2019; Chen and Avissar 1994; Cheng and Cotton 2004; Cioni and Hohenegger 2018; Hong et al. 1995; Mascart et al. 1991). Vegetation-induced solenoidal circulations in tropical continental environments can initiate convection at their edges both by lifting air and by creating a favorable thermodynamic environment (Garcia-Carreras et al. 2011; Taylor et al. 2011). Collisions between solenoidal circulations can also initiate convection (Lynn et al. 1998; Rieck et al. 2014).

Similar to heterogeneous land surfaces, convective cold pools create regions that are favorable for new storm initiation and regions where convection initiation is suppressed. Moist convection tends to be inhibited in the interiors of cold pools (Byers and Braham 1949; Drager and van den Heever 2017). On the other hand, cold pools initiate new storms at their edges through the same mechanisms as solenoidal circulations: mechanical lifting, creating favorable thermodynamics, and collisions (Purdom 1976; Tompkins 2001; Torri et al. 2015; Weaver and Nelson 1982). These similarities suggest that convection initiation may be affected by the interaction between cold pools and solenoidal circulations.

Cold pools and solenoidal circulations can interact in important ways. Cold pools can accelerate or decelerate solenoidal circulations by altering the temperature gradient across the circulation. (Ascher et al. 2024; Harvey et al. 2022; Rieck et al. 2015). Chen et al. (2020) and Ascher et al. (2024) both found that convection which initially forms due to land surface heterogeneities can produce cold pools that subsequently initiate new convection in areas where convection was previously absent. Despite this previous research, the impacts of surface heterogeneity and cold pools on convection initiation have not been systematically disentangled, and the misrepresentation of cold pools and solenoidal circulations is a known source of error in forecast and climate models (Birch et al. 2015; Garcia-Carreras et al. 2013; Rooney et al. 2022; Yang et al. 2021). Studies which aim to understand the impacts of cold pools often conduct mechanism-denial experiments to eliminate cold pools through changes to evaporation (Crook and Moncrieff 1988; Grant et al. 2018, 2020; Jeevanjee and Romps 2013; Khairoutdinov and Randall 2006), but such mechanism-denial experiments are usually conducted over homogeneous surfaces. Recently, Maybee et al. (2025) conducted a mechanism-denial experiment to eliminate cold pools in Sahelian case-study simulations with heterogeneous land surfaces, finding that cold pools were important for the structure of Sahelian MCSs but not for their initiation or maintenance.

The objective of this study is to address the following science question: What are the individual and synergistic impacts of surface heterogeneity/solenoidal circulations and cold pools on convective initiation? We run a set of large eddy simulations (LES) designed to directly address this question. Realistic and weakened cold pools are tested along with realistic and homogenized vegetation. Convective updrafts are tracked to identify where they initiate. Factor separation (Stein and Alpert 1993) is used to disentangle the individual and synergistic impacts of both cold pools and surface heterogeneity on convection initiation.

2 | Methods

2.1 | Large Eddy Simulations

Large eddy simulations are conducted using the Regional Atmospheric Modeling System (RAMS) version 6.3.04 (Cotton et al. 2003; van den Heever et al. 2023; Pielke et al. 1992; Saleeby and van den Heever 2013). Simulations are idealized to isolate processes of interest, except that realistic vegetation data are used to accurately capture the heterogeneity patterns created by deforestation. A horizontal grid spacing of 150 m is used with a timestep of 0.75 s, while the vertical grid spacing starts at 50 m near the surface and is stretched to 300 m. Such grid spacings are necessary to accurately represent cold pools and their interactions with the land surface (Fiévet et al. 2023; Grant and van den Heever 2016; Hirt et al. 2020; Straka et al. 1993). The model domain is 150 × 150 × 24.2 km, is centered at 10.70 S, 62.05 W, and contains the site where the initial sounding was launched from (Figure 1a, where "evergreen broadleaf tree" is rainforest). Periodic lateral boundaries are used. The Land-Ecosystem-Atmosphere-Feedback version 3 (LEAF-3) (Walko et al. 2000) model simulates two-way land-atmosphere interactions. Radiative tendencies are updated every 5 min using Radiative Transfer for Energetics + Rapid Radiative Transfer Model for General circulation model applications—Parallel (RTE + RRTMGP) (Pincus et al. 2019). Cloud microphysics are represented using the RAMS double-moment microphysics scheme (Saleeby and van den Heever 2013).

The atmosphere is initialized using the February 23, 1999 TRMM-LBA sounding presented in Grabowski et al. (2006) (Figure S1). This sounding is chosen because it has been commonly used in studies of Amazon convection and in mechanism-denial studies of cold pools (Grabowski et al. 2006; Khairoutdinov and Randall 2006; Kurowski et al. 2018). Simulations start on February 23, 1999 at 0730 LT (UTC = LT + 4). They are integrated for 5 days to capture multiple diurnal cycles and ensure that large numbers of convective updrafts are simulated, thus generating a statistically robust sample of convection initiation events. Sandy loam soil, an initial soil temperature of 24.8°C, and an initial soil moisture 0.24 $m^3 m^{-3}$ are chosen based on contemporaneous observations shown in Alvalá et al. (2002). The soil extends 2 m below the surface and is broken into 26 levels. Note that all atmospheric and land surface fields are initially horizontally homogeneous in all simulations, other than the vegetation in certain simulations (as described below). Initial random potential temperature perturbations of amplitude 0.1 K in the lowest 500 m are used to facilitate boundary layer development.

Four simulations are conducted to assess the individual and synergistic impacts of land surface heterogeneity and cold pools on convection initiation. In the control simulation (CTRL), realistic vegetation and realistic evaporation are used, thereby representing realistic land surface and cold pool processes. Figure 1a shows the vegetation in CTRL. Note that the vegetation fraction does not vary within each of the three vegetation classes in CTRL. In the homogeneous simulation (HMGN), vegetation properties at each grid point are set to the vegetation-area-weighted mean values of properties in CTRL. Thus, CTRL and HMGN have the same domain-mean vegetation properties, but CTRL has heterogeneously distributed vegetation while HMGN does not. This homogenization only applies to properties which are fixed in time, so prognostic quantities (e.g., soil and canopy moisture/temperature, surface fluxes) are allowed to evolve freely in all simulations. Thus, surface heterogeneities in quantities like soil moisture can develop over time in HMGN. In the evaporation-off simulation (EOFF), evaporation of rain and drizzle are disabled in the lowest 2 km, following Grant et al. (2018). Only the evaporation of falling rain and drizzle are disabled, so other cloud microphysical processes, such as the evaporation of cloud water due to entrainment, remain unaltered. Analysis of density potential temperature at the lowest model level above ground shows that cold pools are almost entirely eliminated in EOFF (Figure S2). Finally, the homogeneous vegetation and evaporation off simulation (HMGN_EOFF) simultaneously applies the homogeneous vegetation of HMGN and the disabled evaporation of EOFF to assess synergistic interactions between these processes.

2.2 | Tracking

We use a tracking algorithm to identify where convective updrafts initiate. By tracking convective updrafts in time, we can

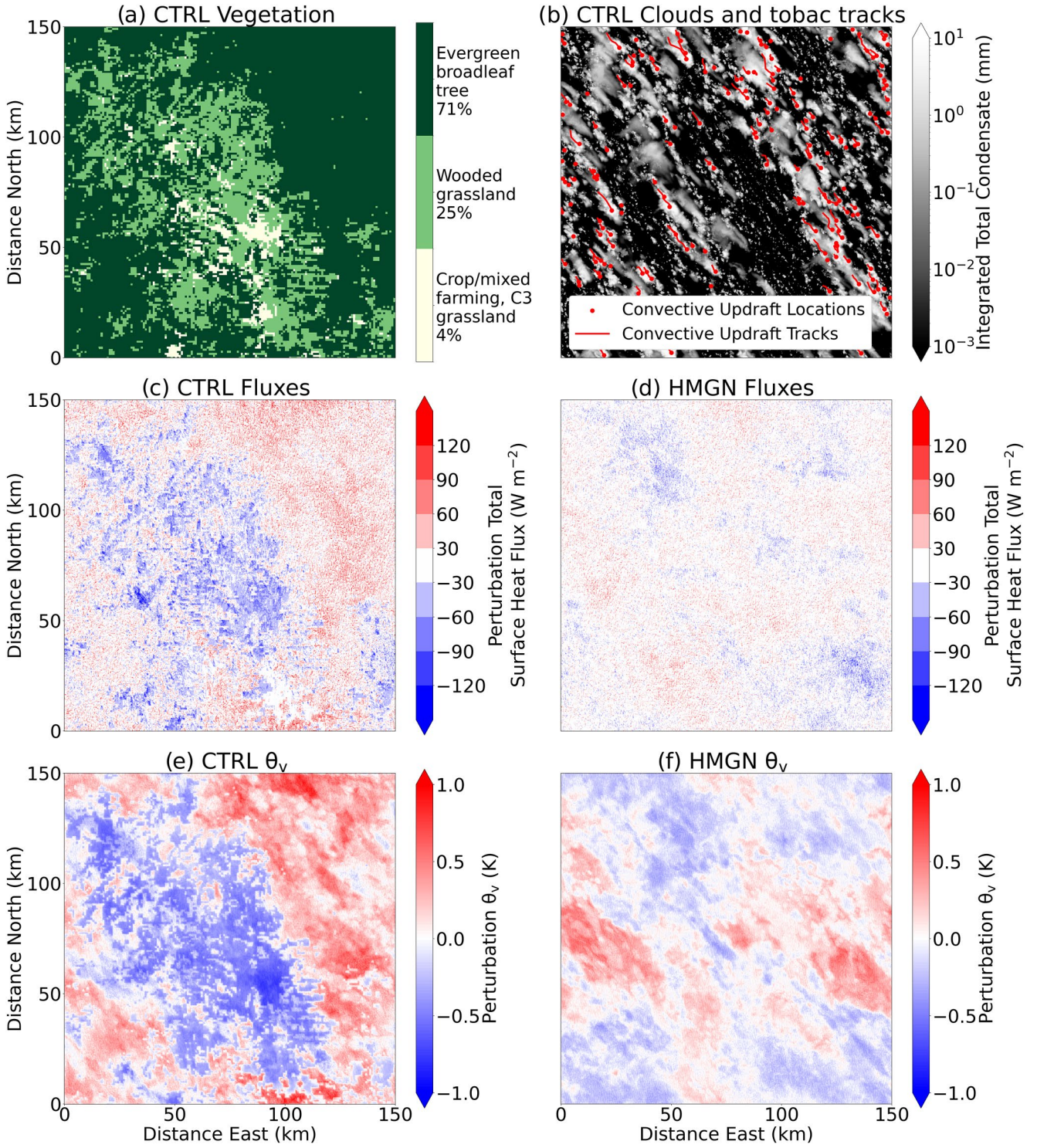

FIGURE 1 | Overview of the basic simulation characteristics. (a) Vegetation class in CTRL (shading) with percent of the domain covered by each class indicated in the colorbar. (b) Vertically integrated total condensate (shading), *tobac*-identified convective updraft locations (red points), and convective updraft tracks (red lines) in CTRL at 1200 LT on day one. (c) Perturbation total surface heat flux (shading) and (e) 25 m AGL perturbation virtual potential temperature (shading) in CTRL. Perturbations are calculated from the domain- and time-mean at 0930 LT across all 5 simulated days. (d, f) As in (c, e) but for HMGN.

distinguish the locations where convective updrafts initiate from the locations where convective updrafts subsequently propagate. We focus our analysis only on the initiation locations of convective updrafts to prevent double-counting. The Tracking and Object-Based Analysis of Clouds (*tobac*) algorithm v1.5 (Heikenfeld et al. 2019; Sokolowsky et al. 2024) is used to track convective updrafts in four dimensions (zonal, meridional, vertical, and time). A vertical velocity threshold of 3 m s^{-1} and a volume threshold of at least 64 contiguous grid points in any spatial dimension is used to identify convective updrafts.

Updrafts tracked for less than 15 min are excluded from further analysis, as updrafts of such durations are likely shallow convection. Updrafts tracked for more than 15 min are referred to as convective updrafts (e.g., Figure 1b, red points and lines). The selected *tobac* thresholds were subjectively determined after trial-and-error, but results are not qualitatively sensitive to the thresholds chosen.

2.3 | Quantifying Aggregation

We use the organization index (I_{org}) (Tompkins and Semie 2017) to quantify the aggregation of convection initiation locations. For a given simulation, the nearest neighbor distances between all convection initiation locations are determined. I_{org} is calculated by plotting the cumulative density function of these nearest neighbor distances (nearest neighbor cumulative density function, or NNCDF) against a NNCDF of random uniform points. The area under this curve is defined as I_{org}. An I_{org} value of ~0.5 indicates the initiation locations are randomly distributed, while values above (below) 0.5 indicate the initiation locations are aggregated (regularly distributed). I_{org} is a dimensionless quantity. All convection initiation locations over the five simulated days are used when calculating I_{org} for a given simulation. We therefore quantify the degree to which the locations where convective updrafts initiate are aggregated. Our use of I_{org} is distinct from past studies that have used I_{org} to quantify the organization of convection at a given snapshot in time (Cheng et al. 2018; Pscheidt et al. 2019; Seifert and Heus 2013). For each simulation, a distribution of I_{org} values is calculated by generating 1000 random uniform NNCDFs and thus recalculating I_{org} 1000 times. For a given simulation X, $I_{org,mean,X}$ represents the mean value of $I_{org,mean,X}$ across these 1000 recalculations.

2.4 | Factor Separation

Factor separation (Stein and Alpert 1993) is applied to understand the individual and synergistic impacts of heterogeneous vegetation and cold pools on patterns of convection initiation. The individual impact of heterogeneous vegetation (F_{VEG}) on I_{org} is calculated as:

$$F_{VEG} = I_{org,mean,EOFF} - I_{org,mean,HMGN\_EOFF}, \quad (1)$$

the individual impact of cold pools (F_{CP}) is calculated as:

$$F_{CP} = I_{org,mean,HMGN} - I_{org,mean,HMGN\_EOFF}, \quad (2)$$

and the impact of synergistic interactions between heterogeneous vegetation and cold pools (F_{VEG_CP}) is calculated as:

$$\begin{aligned} F_{VEG\_CP} &= I_{org,mean,CTRL} - I_{org,mean,HMGN\_EOFF} - F_{VEG} \\ &\quad - F_{CP} = I_{org,mean,CTRL} - \left(I_{org,mean,HMGN} + I_{org,mean,EOFF}\right) \\ &\quad + I_{org,mean,HMGN\_EOFF}. \end{aligned} \quad (3)$$

See Appendix S1 for a detailed explanation of the factor separation method.

3 | Results

Vegetation heterogeneity clearly impacts surface heat fluxes and low-level virtual potential temperature. The total surface heat flux (sum of sensible and latent heat fluxes) at 0930 LT, before deep convection onset, is greater over the forest than the deforested region in CTRL (Figure 1c). Surface heat fluxes are greater over the forest because the surface roughness length is greater and the albedo is smaller over the forested than the deforested region (Table S1). A reduced albedo implies the forest absorbs more energy from solar radiation, while greater roughness lengths mean the forest more efficiently transfers this energy to the atmosphere through turbulent processes. Accordingly, at 0930 LT, the 25 m virtual potential temperature in CTRL is greater over the forest than over the deforested region (Figure 1e). The homogeneous vegetation in HMGN causes perturbations in surface heat fluxes and low-level virtual potential temperature that are smaller in magnitude than in CTRL (compare Figure 1c–f). Perturbations of pre-convective surface heat fluxes and virtual potential temperature in EOFF (HMGN_EOFF) are qualitatively similar to those for CTRL (HMGN) (not shown).

Convective updrafts in CTRL and EOFF initiate less frequently over the deforested region than over the forest (Figure 2a,c). The lack of convective updrafts in the deforested region can be explained by the reduced virtual potential temperature, and hence the air being less buoyant, compared to the forest (Figure 1a,e). At low-levels, the forest is warmer but slightly drier than the deforested region (Figure S3), a response to deforestation which has been shown to occur in tropical regions with high soil moisture (van der Molen et al. 2006). The forest is drier than the deforested region at low-levels partially due to enhanced vertical mixing of moisture over the forest (Figure S3d). The locations of convection initiation before 1200 LT in CTRL and EOFF demonstrate the effects of vegetation-driven solenoidal circulations and cold pools on convective updraft initiation (Figure 2b,d). During this time period, convection initiates most frequently near the forested-deforested boundary. These patterns are consistent with solenoidal circulations beginning to propagate from the deforested region into the forest and initiating convection. As the day progresses, these solenoidal circulations propagate further into the forested region and continue to initiate convection (not shown). Therefore, while solenoidal circulations are evident in the simulations, their effects are muted in Figure 2a,c because the entire diurnal cycle is shown and the effects of the solenoidal circulations are spread across the forest.

Convective updrafts in HMGN and HMGN_EOFF initiate more uniformly across the domain than convective updrafts in CTRL and EOFF (Figure 2a,c,e,f). Virtual potential temperature is more uniform across the domain with homogeneous vegetation compared to heterogeneous vegetation (Figure 1e,f). Therefore, convection initiation is not favored nor disfavored in specific regions, nor can solenoidal circulations form in the homogeneous vegetation simulations.

Cold pools also influence where convection initiates. Recall the only difference between EOFF and CTRL is the suppressed evaporation of precipitation in the lowest 2 km, and therefore lack of cold pools, in EOFF. Convective updrafts in EOFF initiate less

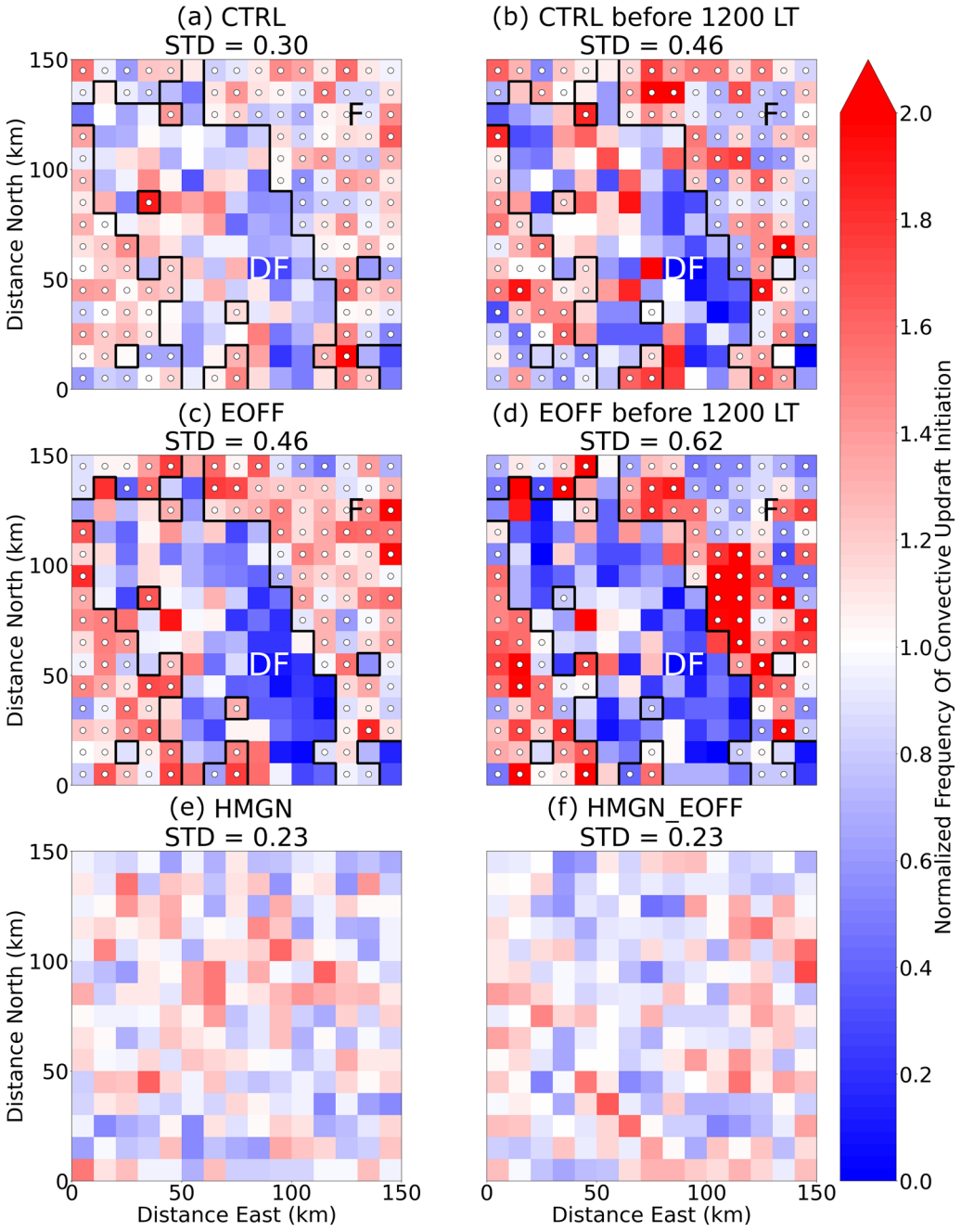

FIGURE 2 | Convective updrafts initiate more frequently over forested than deforested areas, especially when cold pools are not present. (a, c, e, f) Heatmaps of convection initiation locations for CTRL, EOFF, HMGN, and HMGN_EOFF, respectively; values are normalized such that 1.0 is the domain mean for each panel, and a value of 2.0 represents twice the number of initiating convective updrafts compared to 1.0. (b, d) as in (a, c) but only for convective updrafts which initiate between 0000 LT and 1155 LT. White dots indicate bins with more forest cover than the domain mean (71%). Black contours separate forested and deforested areas. Labels F (DF) also indicate forest (deforested region). The standard deviation of plotted values is included in the title of each panel.

frequently over the deforested region than convective updrafts in CTRL (compare Figure 2a,c). This suggests that cold pools in CTRL propagate from the forest into the deforested region and initiate convective updrafts over the deforested region, despite the less favorable conditions for convection initiation compared to the forest. On the other hand, in EOFF, very few convective updrafts initiate in the deforested region due to the lack of cold pool-induced initiation. To further support this argument, we return to Figure 2b. The time period shown captures the first set of convective updrafts on each day in CTRL which initiate before strong cold pools form, thus partially removing the influence of cold pools. Early convection initiation frequency in CTRL is suppressed in the deforested region relative to later time periods (compare Figure 2a,b) and even approaches the magnitude of suppression in EOFF over the full diurnal cycle (compare Figure 2b,c), further demonstrating that cold pools are largely responsible for the initiation of convective updrafts in the deforested region of CTRL.

To investigate the mechanisms driving convective initiation, we create composites of low-level density potential temperature,

water vapor mixing ratio, and vertical velocity around each convective updraft initiation. We further categorize each convective updraft initiation based on whether it occurs near no, one, or multiple density currents (cold pools and/or solenoidal circulations) (Figure 3). Composites are rotated so that density currents are on the left side of each panel in Figure 3, and flipped so that colliding density currents are on the bottom right of each panel in Figure 3c,f,i,l. Appendix S2 describes the procedure for categorization and compositing in detail. Cold pools play a major role in initiating convection, as density currents initiate ~58% of convective updrafts in HMGN (Figure 3e,f), where cold pools are present, but only ~9% of convective updrafts in HMGN_EOFF, where cold pools are absent (Figure 3k,l). Solenoidal circulations play a secondary role, as ~14% of convective updrafts are initiated by one or more density currents in EOFF (Figure 3h,i), compared to ~9% in HMGN_EOFF (Figure 3k,l). Regardless of the simulation, density currents are associated with enhanced water vapor mixing ratio and vertical velocity at their edges (Figure 3), which previous studies have shown can lead to the initiation of new convection (Garcia-Carreras et al. 2011; Purdom 1976; Tompkins 2001). Note that some density currents are still present in HMGN_EOFF (Figure 3j–l) as cold pools are weakened, but not completely eliminated, in this simulation and in EOFF.

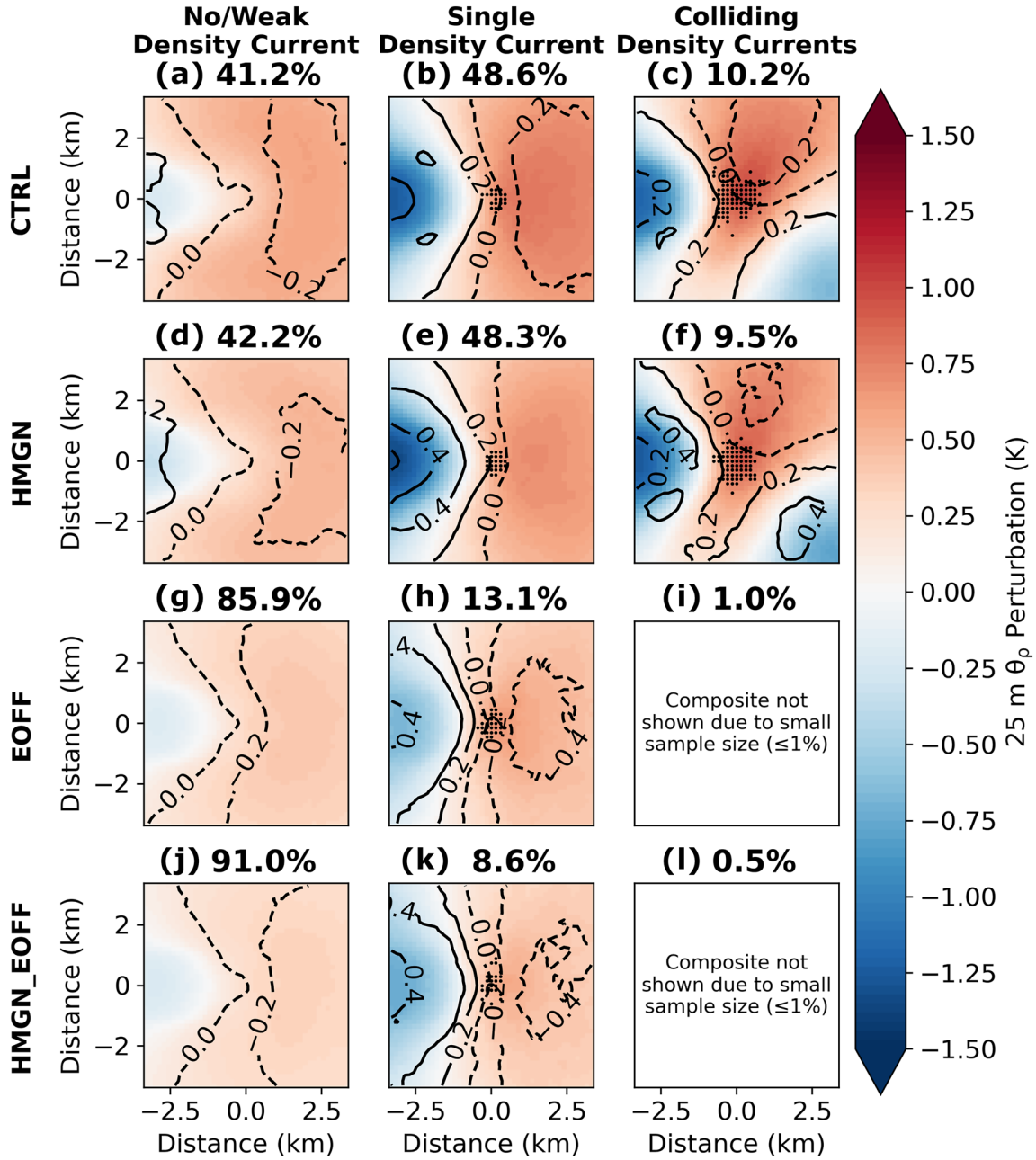

FIGURE 3 | Density currents initiate convection by enhancing water vapor mixing ratio and vertical velocity. Composites of density potential temperature perturbation at 25 m AGL (shading), water vapor mixing ratio perturbation at 25 m AGL (contours every 0.2 g kg^{-1}), and vertical velocity at 50 m AGL (black stippling for values greater than 0.1 m s^{-1}) centered over convection initiation locations for each simulation (rows) and density current category (rows). The title of each panel indicates the percentage of initiations in the given category for the given simulation.

We now use I_{org} to quantify the impact of heterogeneous vegetation and cold pools on convection initiation locations (Figure 4a). Convective updrafts are close to randomly distributed with homogeneous vegetation, as the mean I_{org} for HMGN and HMGN_EOFF are both ~0.5 (Figure 4a). The individual effect of cold pools (F_{CP}) on I_{org} is small compared to the individual effect of vegetation heterogeneity (F_{VEG}) and the synergistic interactions between vegetation patterns and cold pools (F_{VEG_CP}) (Figure 4c), demonstrating that cold pools do not have a large impact on the randomness of convection initiation locations over homogeneous vegetation (Figures 2e,f and 4a). Heterogeneous vegetation acts to aggregate convection initiation locations, since F_{VEG} is positive for mean I_{org} (Figure 4c), consistent with our previous finding that convection initiation is less frequent over the deforested regions of CTRL and EOFF than the forests. The synergistic interactions between heterogeneous vegetation and cold pools act to disaggregate convection initiation locations, since F_{VEG_CP} is negative for I_{org} (Figure 4c), consistent with cold pools propagating from the forest into the deforested regions and subsequently initiating convection in the deforested region of CTRL but not in EOFF. Thus, the effects of cold pools on convection initiation patterns are only apparent when vegetation is heterogeneous. Each distribution shown in Figure 4a is significantly different from the other distributions at the $p < 0.001$ level.

Precipitation is impacted by changes in convection initiation driven by heterogeneous vegetation and cold pools. Figure 4b (3d) shows precipitation in CTRL (EOFF), normalized by the domain mean precipitation to account for the differences in evaporation processes between CTRL and EOFF. The downwind (southeast) portion of the deforested region of EOFF receives almost no precipitation (Figure 4d), while such a pattern is less evident in CTRL (Figure 4b). These precipitation patterns follow from patterns in convection initiation and the generally southeastward motion of convective updrafts (Figures 1b and 2). We define "precipitation gaps" as areas of the domain receiving < 1 mm of precipitation. We determine the total area of precipitation gaps in each simulation and conduct factor separation analysis on this metric in an analogous manner as it is

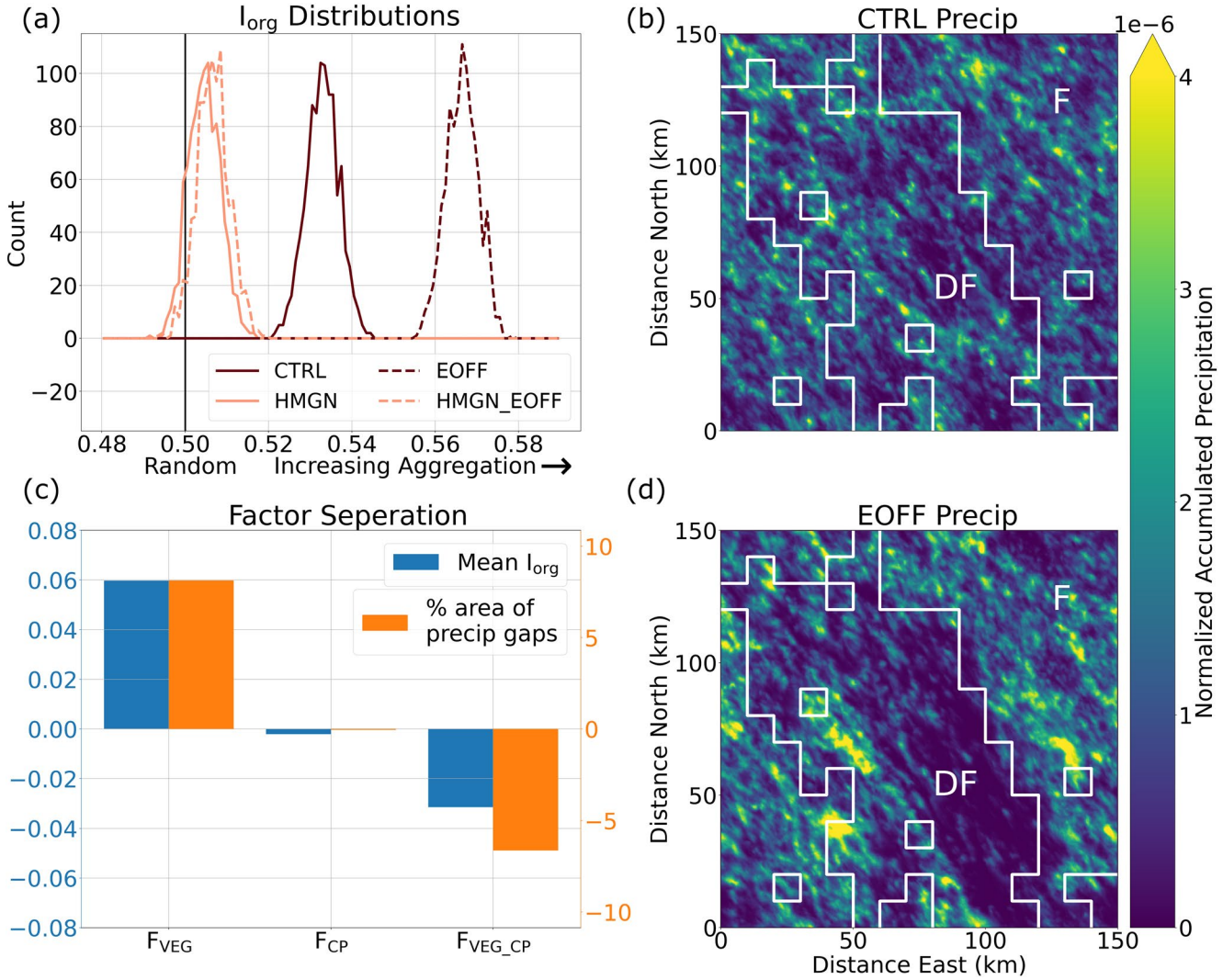

FIGURE 4 | Cold pools disaggregate convection initiation locations and accumulated precipitation over heterogeneous vegetation. (a) Distributions of I_{org} of convection initiation locations for each simulation. (b, d) Normalized accumulated precipitation over the five simulated days (shading) for (b) CTRL and (d) EOFF where text and white contour indicate forested and deforested areas. (c) Factor separation analysis of mean I_{org} values and percentage area of precipitation gaps.

conducted for I_{org} (Figure 4c). The factors for this precipitation gap metric have similar relative magnitudes as the factors for mean I_{org}, thereby demonstrating that aggregating (disaggregating) convective initiation locations causes precipitation gaps to become larger (smaller).

4 | Summary and Conclusions

This study aimed to investigate the individual and synergistic impacts of surface heterogeneity and cold pools on the initiation of tropical continental convective storms. We find that greater surface roughness and lower albedo lead to greater surface heat fluxes and virtual potential temperatures over forested compared to deforested regions (Figure 1a,c,e). This results in more frequent convection initiation over forests than deforested regions due to favorable thermodynamics and the development of solenoidal circulations near forested and deforested boundaries (Figure 2a–d). Convection initiation locations are therefore aggregated over heterogeneous vegetation (Figure 4a). However, similar to findings by Chen et al. (2020) and Ascher et al. (2024), cold pools can propagate away from convective updrafts over the forest and initiate new convection over the less thermodynamically favorable deforested region (Figure 2a–d). This mechanism partially counteracts the effects of heterogeneous vegetation and disaggregates convection initiation locations (Figure 4a,c). Without cold pools, a large gap in the precipitation field forms over the deforested region in the heterogeneous vegetation simulation, since few convective updrafts initiate in this region (Figure 2c, Figure 4d). Convection initiation is nearly random over homogeneous vegetation, regardless of whether or not cold pools are present, so the disaggregating effect of cold pools on convection initiation locations is only important for heterogeneous vegetation (Figures 2e,f and 4a).

The results of this study indicate that interactions between heterogeneous surfaces and cold pools are crucial for convection initiation patterns. While our simulations are representative of convection in the Amazon rainforest, we suggest that cold pools can similarly counteract the effects of heterogeneous vegetation in other environments. Accurately parameterizing interactions between heterogeneous surfaces and cold pools may improve the ability of forecast and climate models to represent convection initiation over heterogeneous surfaces. While not tested in this study, the background wind, which was coincidentally perpendicular to the solenoidal circulations, likely plays an important role (Allouche et al. 2023; Findell and Eltahir 2003a, 2003b) and should be tested. This study focused on scattered convection, but results may differ for organized systems, as Maybee et al. (2025) found that Sahelian MCS initiation rates are slightly increased in a simulation with suppressed cold pools. Finally, an important takeaway from this study is that, while deforestation and other land use changes may impact the distribution of precipitation in certain regions, cold pools partially counteract these changes.

Author Contributions

Nicholas M. Falk: conceptualization, data curation, formal analysis, methodology, software, visualization, writing – original draft, writing – review and editing. **Gabrielle R. Leung:** formal analysis, methodology, software, writing – review and editing. **Leah D. Grant:** conceptualization, formal analysis, funding acquisition, resources, supervision, writing – review and editing. **Susan C. van den Heever:** conceptualization, formal analysis, funding acquisition, resources, supervision, writing – review and editing.

Acknowledgments

Funding was provided by NSF Grant AGS-2029611. G.R.L. acknowledges funding by the NASA Early Career Research program through FINESST 80NSSC22K1446. We would like to acknowledge high-performance computing support from the Derecho system (https://doi.org/10.5065/qx9a-pg09) provided by the NSF National Center for Atmospheric Research (NCAR), sponsored by the National Science Foundation. We thank Dr. Aryeh Drager for helpful discussions pertaining to land surface processes in RAMS. We also thank the two anonymous reviewers for their insightful and constructive comments.

Funding

This work was supported by National Science Foundation (NSF) (grant AGS-2029611). G.R.L. acknowledges funding by the National Aeronautics and Space Administration (NASA) Early Career Research program through FINESST 80NSSC22K1446.

Conflicts of Interest

The authors declare no conflicts of interest.

Data Availability Statement

Model source code, name lists, and analysis scripts are available at: https://doi.org/10.5281/zenodo.17654571.

References

Allouche, M., E. Bou-Zeid, and J. Iipponen. 2023. "The Influence of Synoptic Wind on Land–Sea Breezes." *Quarterly Journal of the Royal Meteorological Society* 149, no. 757: 3198–3219.

Alvalá, R. C. S., R. Gielow, H. R. da Rocha, et al. 2002. "Intradiurnal and Seasonal Variability of Soil Temperature, Heat Flux, Soil Moisture Content, and Thermal Properties Under Forest and Pasture in Rondônia." *Journal of Geophysical Research: Atmospheres* 107, no. D20: LBA 10-1–LBA 10-20.

Ascher, B. D., S. M. Saleeby, P. J. Marinescu, and S. C. van den Heever. 2024. "Forest Breeze–Cold Pool Interactions Drive Convective Organization Over Heterogeneous Vegetation." *Journal of the Atmospheric Sciences* 82: 71–94. https://doi.org/10.1175/JAS-D-24-0084.1.

Birch, C. E., M. J. Roberts, L. Garcia-Carreras, et al. 2015. "Sea-Breeze Dynamics and Convection Initiation: The Influence of Convective Parameterization in Weather and Climate Model Biases." *Journal of Climate* 28, no. 20: 8093–8108.

Branch, O., and V. Wulfmeyer. 2019. "Deliberate Enhancement of Rainfall Using Desert Plantations." *Proceedings of the National Academy of Sciences* 116, no. 38: 18841–18847.

Byers, H. R., and R. R. Braham. 1949. *The Thunderstorm: Report of the Thunderstorm Project*. U.S. Government Printing Office.

Chagnon, F. J. F., R. L. Bras, and J. Wang. 2004. "Climatic Shift in Patterns of Shallow Clouds Over the Amazon." *Geophysical Research Letters* 31, no. 24: L24212. https://doi.org/10.1029/2004GL021188.

Chen, F., and R. Avissar. 1994. "Impact of Land-Surface Moisture Variability on Local Shallow Convective Cumulus and Precipitation in Large-Scale Models." *Journal of Applied Meteorology* 33, no. 12: 1382–1401.

Chen, J., S. Hagos, H. Xiao, J. D. Fast, and Z. Feng. 2020. "Characterization of Surface Heterogeneity-Induced Convection Using Cluster Analysis." *Journal of Geophysical Research: Atmospheres* 125, no. 20: e2020JD032550.

Cheng, W. Y. Y., and W. R. Cotton. 2004. "Sensitivity of a Cloud-Resolving Simulation of the Genesis of a Mesoscale Convective System to Horizontal Heterogeneities in Soil Moisture Initialization." *Journal of Hydrometeorology* 5, no. 5: 934–958.

Cheng, W.-Y., D. Kim, and A. Rowe. 2018. "Objective Quantification of Convective Clustering Observed During the AMIE/DYNAMO Two-Day Rain Episodes." *Journal of Geophysical Research* 123, no. 18: 10,361–10,378.

Cioni, G., and C. Hohenegger. 2018. "A Simplified Model of Precipitation Enhancement Over a Heterogeneous Surface." *Hydrology and Earth System Sciences* 22, no. 6: 3197–3212.

Cotton, W. R., R. A. Pielke Sr., R. L. Walko, et al. 2003. "RAMS 2001: Current Status and Future Directions." *Meteorology and Atmospheric Physics* 82, no. 1: 5–29.

Crook, N. A., and M. W. Moncrieff. 1988. "The Effect of Large-Scale Convergence on the Generation and Maintenance of Deep Moist Convection." *Journal of the Atmospheric Sciences* 45, no. 23: 3606–3624.

Drager, A. J., and S. C. van den Heever. 2017. "Characterizing Convective Cold Pools." *Journal of Advances in Modeling Earth Systems* 9, no. 2: 1091–1115.

Durieux, L., L. A. T. Machado, and H. Laurent. 2003. "The Impact of Deforestation on Cloud Cover Over the Amazon Arc of Deforestation." *Remote Sensing of Environment* 86, no. 1: 132–140.

Fiévet, R., B. Meyer, and J. O. Haerter. 2023. "On the Sensitivity of Convective Cold Pools to Mesh Resolution." *Journal of Advances in Modeling Earth Systems* 15, no. 8: e2022MS003382.

Findell, K. L., and E. A. B. Eltahir. 2003a. "Atmospheric Controls on Soil Moisture–Boundary Layer Interactions. Part I: Framework Development." *Journal of Hydrometeorology* 4, no. 3: 552–569.

Findell, K. L., and E. A. B. Eltahir. 2003b. "Atmospheric Controls on Soil Moisture–Boundary Layer Interactions: Three-Dimensional Wind Effects." *Journal of Geophysical Research: Atmospheres* 108, no. D8: 8385. https://doi.org/10.1029/2001JD001515.

Garcia-Carreras, L., J. H. Marsham, D. J. Parker, et al. 2013. "The Impact of Convective Cold Pool Outflows on Model Biases in the Sahara." *Geophysical Research Letters* 40, no. 8: 1647–1652.

Garcia-Carreras, L., D. J. Parker, and J. H. Marsham. 2011. "What Is the Mechanism for the Modification of Convective Cloud Distributions by Land Surface–Induced Flows?" *Journal of the Atmospheric Sciences* 68, no. 3: 619–634.

Grabowski, W. W., P. Bechtold, A. Cheng, et al. 2006. "Daytime Convective Development Over Land: A Model Intercomparison Based on LBA Observations." *Quarterly Journal of the Royal Meteorological Society* 132, no. 615: 317–344.

Grant, L. D., T. P. Lane, and S. C. van den Heever. 2018. "The Role of Cold Pools in Tropical Oceanic Convective Systems." *Journal of the Atmospheric Sciences* 75, no. 8: 2615–2634.

Grant, L. D., M. W. Moncrieff, T. P. Lane, and S. C. van den Heever. 2020. "Shear-Parallel Tropical Convective Systems: Importance of Cold Pools and Wind Shear." *Geophysical Research Letters* 47, no. 12: e2020GL087720.

Grant, L. D., and S. C. van den Heever. 2016. "Cold Pool Dissipation." *Journal of Geophysical Research. Atmospheres* 121, no. 3: 1138–1155.

Harvey, N. J., C. L. Daleu, R. A. Stratton, R. S. Plant, S. J. Woolnough, and A. J. Stirling. 2022. "The Impact of Surface Heterogeneity on the Diurnal Cycle of Deep Convection." *Quarterly Journal of the Royal Meteorological Society* 148, no. 749: 3509–3527.

Heikenfeld, M., P. J. Marinescu, M. Christensen, et al. 2019. "Tobac 1.2: Towards a Flexible Framework for Tracking and Analysis of Clouds in Diverse Datasets." *Geoscientific Model Development* 12, no. 11: 4551–4570.

Hirt, M., G. C. Craig, S. A. K. Schäfer, J. Savre, and R. Heinze. 2020. "Cold-Pool-Driven Convective Initiation: Using Causal Graph Analysis to Determine What Convection-Permitting Models Are Missing." *Quarterly Journal of the Royal Meteorological Society* 146, no. 730: 2205–2227.

Hong, X., M. J. Leach, and S. Raman. 1995. "A Sensitivity Study of Convective Cloud Formation by Vegetation Forcing With Different Atmospheric Conditions." *Journal of Applied Meteorology* 34, no. 9: 2008–2028.

Jeevanjee, N., and D. M. Romps. 2013. "Convective Self-Aggregation, Cold Pools, and Domain Size." *Geophysical Research Letters* 40, no. 5: 994–998.

Khairoutdinov, M., and D. Randall. 2006. "High-Resolution Simulation of Shallow-to-Deep Convection Transition Over Land." *Journal of the Atmospheric Sciences* 63, no. 12: 3421–3436.

Kurowski, M. J., K. Suselj, W. W. Grabowski, and J. Teixeira. 2018. "Shallow-to-Deep Transition of Continental Moist Convection: Cold Pools, Surface Fluxes, and Mesoscale Organization." *Journal of the Atmospheric Sciences* 75, no. 12: 4071–4090.

Lynn, B. H., W.-K. Tao, and P. J. Wetzel. 1998. "A Study of Landscape-Generated Deep Moist Convection." *Monthly Weather Review* 126, no. 4: 928–942.

Mascart, P., O. Taconet, J.-P. Pinty, and M. B. Mehrez. 1991. "Canopy Resistance Formulation and Its Effect in Mesoscale Models: A HAPEX Perspective." *Agricultural and Forest Meteorology* 54, no. 2: 319–351.

Maybee, B., J. Bassford, J. H. Marsham, et al. 2025. "How Sensitive Are Sahelian Mesoscale Convective Systems to Cold-Pool Suppression?" *Quarterly Journal of the Royal Meteorological Society* 151, no. 772: e5032.

Paccini, L., and K. A. Schiro. 2025. "Influence of Soil Moisture on the Development of Organized Convective Systems in South America." *Journal of Geophysical Research: Atmospheres* 130, no. 9: e2024JD042108.

Pielke, R. A., W. R. Cotton, R. L. Walko, et al. 1992. "A Comprehensive Meteorological Modeling System—RAMS." *Meteorology and Atmospheric Physics* 49, no. 1: 69–91.

Pincus, R., E. J. Mlawer, and J. S. Delamere. 2019. "Balancing Accuracy, Efficiency, and Flexibility in Radiation Calculations for Dynamical Models." *Journal of Advances in Modeling Earth Systems* 11, no. 10: 3074–3089.

Pscheidt, I., F. Senf, R. Heinze, H. Deneke, S. Trömel, and C. Hohenegger. 2019. "How Organized Is Deep Convection Over Germany?" *Quarterly Journal of the Royal Meteorological Society* 145, no. 723: 2366–2384.

Purdom, J. F. W. 1976. "Some Uses of High-Resolution GOES Imagery in the Mesoscale Forecasting of Convection and Its Behavior." *Monthly Weather Review* 104, no. 12: 1474–1483.

Rabin, R. M., S. Stadler, P. J. Wetzel, D. J. Stensrud, and M. Gregory. 1990. "Observed Effects of Landscape Variability on Convective Clouds." *Bulletin of the American Meteorological Society* 71, no. 3: 272–280.

Rieck, M., C. Hohenegger, and P. Gentine. 2015. "The Effect of Moist Convection on Thermally Induced Mesoscale Circulations." *Quarterly Journal of the Royal Meteorological Society* 141, no. 691: 2418–2428.

Rieck, M., C. Hohenegger, and C. C. van Heerwaarden. 2014. "The Influence of Land Surface Heterogeneities on Cloud Size Development." *Monthly Weather Review* 142, no. 10: 3830–3846.

Rooney, G. G., A. J. Stirling, R. A. Stratton, and M. Whitall. 2022. "C-POOL: A Scheme for Modelling Convective Cold Pools in the Met Office

Unified Model." *Quarterly Journal of the Royal Meteorological Society* 148, no. 743: 962–980.

Saleeby, S. M., and S. C. van den Heever. 2013. "Developments in the CSU-RAMS Aerosol Model: Emissions, Nucleation, Regeneration, Deposition, and Radiation." *Journal of Applied Meteorology and Climatology* 52, no. 12: 2601–2622.

Seifert, A., and T. Heus. 2013. "Large-Eddy Simulation of Organized Precipitating Trade Wind Cumulus Clouds." *Atmospheric Chemistry and Physics* 13, no. 11: 5631–5645.

Sokolowsky, G. A., S. W. Freeman, W. K. Jones, et al. 2024. "Textittobac v1.5: Introducing Fast 3D Tracking, Splits and Mergers, and Other Enhancements for Identifying and Analysing Meteorological Phenomena." *Geoscientific Model Development* 17, no. 13: 5309–5330.

Souza, E. P., N. O. Rennó, and M. A. F. S. Dias. 2000. "Convective Circulations Induced by Surface Heterogeneities." *Journal of the Atmospheric Sciences* 57, no. 17: 2915–2922.

Stein, U., and P. Alpert. 1993. "Factor Separation in Numerical Simulations." *Journal of the Atmospheric Sciences* 50, no. 14: 2107–2115.

Straka, J. M., R. B. Wilhelmson, L. J. Wicker, J. R. Anderson, and K. K. Droegemeier. 1993. "Numerical Solutions of a Non-Linear Density Current: A Benchmark Solution and Comparisons." *International Journal for Numerical Methods in Fluids* 17, no. 1: 1–22.

Taylor, C. M., R. A. M. de Jeu, F. Guichard, P. P. Harris, and W. A. Dorigo. 2012. "Afternoon Rain More Likely Over Drier Soils." *Nature* 489, no. 7416: 423–426.

Taylor, C. M., A. Gounou, F. Guichard, et al. 2011. "Frequency of Sahelian Storm Initiation Enhanced Over Mesoscale Soil-Moisture Patterns." *Nature Geoscience* 4, no. 7: 430–433.

Tompkins, A. M. 2001. "Organization of Tropical Convection in Low Vertical Wind Shears: The Role of Cold Pools." *Journal of the Atmospheric Sciences* 58, no. 13: 1650–1672.

Tompkins, A. M., and A. G. Semie. 2017. "Organization of Tropical Convection in Low Vertical Wind Shears: Role of Updraft Entrainment." *Journal of Advances in Modeling Earth Systems* 9, no. 2: 1046–1068.

Torri, G., Z. Kuang, and Y. Tian. 2015. "Mechanisms for Convection Triggering by Cold Pools." *Geophysical Research Letters* 42, no. 6: 1943–1950.

van den Heever, S. C., S. M. Saleeby, L. D. Grant, A. L. Igel, and S. W. Freeman. 2023. "RAMS—The Regional Atmospheric Modeling System (Version v6.3.04)." *Zenodo*. https://doi.org/10.5281/zenodo.8327421.

van der Molen, M. K., A. J. Dolman, M. J. Waterloo, and L. A. Bruijnzeel. 2006. "Climate Is Affected More by Maritime Than by Continental Land Use Change: A Multiple Scale Analysis." *Global and Planetary Change* 54, no. 1: 128–149.

Walko, R. L., L. E. Band, J. Baron, et al. 2000. "Coupled Atmosphere–Biophysics–Hydrology Models for Environmental Modeling." *Journal of Applied Meteorology and Climatology* 39, no. 6: 931–944.

Wang, J., F. J. F. Chagnon, E. R. Williams, et al. 2009. "Impact of Deforestation in the Amazon Basin on Cloud Climatology." *Proceedings of the National Academy of Sciences* 106, no. 10: 3670–3674.

Weaver, J. F., and S. P. Nelson. 1982. "Multiscale Aspects of Thunderstorm Gust Fronts and Their Effects on Subsequent Storm Development." *Monthly Weather Review* 110, no. 7: 707–718.

Yang, B., M. Wang, G. J. Zhang, et al. 2021. "Linking Deep and Shallow Convective Mass Fluxes via an Assumed Entrainment Distribution in CAM5-CLUBB: Parameterization and Simulated Precipitation Variability." *Journal of Advances in Modeling Earth Systems* 13, no. 5: e2020MS002357.

Supporting Information

Additional supporting information can be found online in the Supporting Information section. **Data S1:** asl270011-sup-0001-Supinfo01.docx.